



Improved detection of focal cortical dysplasia using a novel 3D imaging sequence: Edge-Enhancing Gradient Echo (3D-EDGE) MRI

Erik H. Middlebrooks^{a,b,*}, Chen Lin^a, Erin Westerhold^a, Lela Okromelidze^a, Prasanna Vibhute^a, Sanjeet S. Grewal^b, Vivek Gupta^a

^a Department of Radiology, Mayo Clinic, Jacksonville, FL, USA

^b Department of Neurosurgery, Mayo Clinic, Jacksonville, FL, USA

ARTICLE INFO

Keywords:

Epilepsy
Seizures
Focal cortical dysplasia
MRI

ABSTRACT

Epilepsy is a common neurological disorder with focal cortical dysplasia (FCD) being one of the most common lesional causes. Detection of FCD by MRI is a major determinant of surgical outcome. Evolution of MRI sequences and hardware has greatly increased the detection rate of FCD, but these gains have largely been related to the more visible Type IIb FCD, with Type I and IIa remaining elusive. While most sequence improvements have relied on increasing contrast between gray and white matter, we propose a novel imaging approach, 3D Edge-Enhancing Gradient Echo (3D-EDGE), to directly image the gray-white boundary. By acquiring images at an inversion time where gray and white matter have equal signal but opposite phases, voxels with a mixture of gray and white matter (e.g., at the gray-white boundary) will have cancellation of longitudinal magnetization producing a thin area of signal void at the normal boundary. By creating greater sensitivity for minor changes in T1 relaxation, microarchitectural abnormalities present in FCD produce greater contrast than on other common MRI sequences. 3D-EDGE had a significantly greater contrast ratio between lesion and white matter for FCD compared to MP2RAGE (98% vs 17%; $p = 0.0006$) and FLAIR (98% vs 19%; $p = 0.0006$), which highlights its potential to improve outcomes in epilepsy. We present a discussion of the framework for 3D-EDGE, optimization strategies, and analysis of a series of FCDs to highlight the benefit of 3D-EDGE in FCD detection compared to commonly used sequences in epilepsy.

1. Introduction

Epilepsy is a frequent cause of disability and death throughout the world despite continued advances in diagnosis and treatment. Of patients with epilepsy, 20%–40% are defined as drug-refractory and may be candidates for surgical treatment (Engel et al., 2012). Unfortunately, surgical outcomes are highly variable, and detecting an epileptogenic lesion on neuroimaging is a major contributor to treatment success or failure. In fact, MRI-negative cases of epilepsy have shown 38–46% seizure freedom (Engel class I) compared to nearly 80% of MRI-positive cases (Bien et al., 2009; Shi et al., 2017; Immonen et al., 2010). Likewise, more than half of MRI-negative cases had poor outcomes (Engel class III–IV) (Immonen et al., 2010). Patients with MRI-negative epilepsy are also far less frequently offered surgical treatment (Bien et al., 2009).

Advances in MRI technology have greatly aided in the detection of

epileptogenic lesions, particularly with increased detection of hippocampal sclerosis and migrational abnormalities. Routine use of higher field strength MRI, namely 3 Tesla (T) scanners, has been shown to increase lesion detection by an odds ratio of greater than 2.5 compared to 1.5 T (Phal et al., 2008) and also allows significantly improved delineation of hippocampal subfields for detection of subtle hippocampal sclerosis (Middlebrooks et al., 2017). Recent FDA approval of 7 T MRI for clinical use is another major step in improving lesion detection, with even further increase in lesion detection compared to 3 T (De Ciantis et al., 2016). Improvements in imaging sequences have also aided lesion detection, such as Magnetization Prepared Rapid Acquisition Gradient Echo with two inversion times (MP2RAGE) (Marques et al., 2010), Double Inversion Recovery (DIR) (Boulby et al., 2004), and Fluid and White Matter Suppression (FLAWS) MRI (Chen et al., 2018). Despite these advances, detection rates remain quite low for cortical migration

Abbreviations: 3D-EDGE, 3D Edge-Enhancing Gradient Echo; DIR, Double Inversion Recovery; FCD, focal cortical dysplasia; GM, gray matter; MP2RAGE, Magnetization Prepared Rapid Acquisition Gradient Echo with two inversion times; WM, white matter.

* Corresponding author at: Department of Radiology, Mayo Clinic, Jacksonville, FL, USA.

E-mail address: middlebrooks.erik@mayo.edu (E.H. Middlebrooks).

<https://doi.org/10.1016/j.nicl.2020.102449>

Received 18 August 2020; Received in revised form 18 September 2020; Accepted 22 September 2020

Available online 28 September 2020

2213-1582/© 2020 The Author(s).

Published by Elsevier Inc.

This is an open access article under the CC BY-NC-ND license

(<http://creativecommons.org/licenses/by-nc-nd/4.0/>).

abnormalities, in particular focal cortical dysplasia (FCD). Specifically, Type I and Type IIa FCDs have a much higher association with MRI-negative epilepsy due to their difficulty in detection compared with Type IIb FCD, which more commonly manifests with greater gray matter (GM) thickening, subcortical white matter (WM) signal abnormality, and blurring of the GM-WM boundary (Lerner et al., 2009).

To date, many commonly used sequences have focused on optimization of contrast between GM and WM (Middlebrooks et al., 2017). While the increased contrast has improved detection of FCDs, especially Type IIb FCDs, more subtle abnormalities of the GM-WM boundary remain elusive. Our goal was to pursue a different approach of directly imaging the GM-WM boundary using a novel 3D MRI contrast, Edge-Enhancing Gradient Echo (3D-EDGE), in attempt to increase the conspicuity of FCDs in the evaluation of epilepsy. We present a framework for this novel sequence, as well as optimization strategies and clinical case examples.

2. Methods

2.1. Theory

GM largely consists of layers of densely packed neuronal cell bodies with relatively little myelin content, while the adjacent WM predominantly contains myelinated axons. In order to directly visualize and detect abnormalities of the GM-WM boundary, the inversion time (TI) in the 3D-EDGE sequence is optimized for GM and WM to have comparable signal intensity, but with opposite polarity of longitudinal magnetization (Fig. 1). Due to volume averaging in MRI, the normal GM-WM boundary consists of voxels sharing a variable percentage of both GM and WM (Fig. 2A & B). Under this condition, GM and WM signals cancel each other at the normal GM-WM boundary, producing a narrow strip or curve of signal void. This is similar to the dark line at fat and water interfaces, where fat and water signals cancel each other when the TE time in a gradient echo sequence matches one of the TEs with opposed phase transverse magnetizations of fat and water. We hypothesize that areas with alterations in the normal composition of GM and WM, and therefore the T1 relaxation, at the GM-WM boundary will produce disruption or thickening of the narrow signal void in those regions.

A common manifestation of FCD involves abnormalities of the GM-WM boundary (Fig. 2C). Abnormal lamination in FCD, resulting in alterations in neuronal and axonal density, can affect normal T1 values in the tissue (Blackmon et al., 2015). Additionally, increased density of

interstitial neurons in white matter immediately deep to the inner cortical layer, as a consequence of arrested migration and cortical organization, results in slight prolongation of T1 in white matter voxels near the GM-WM boundary (Blackmon et al., 2015). While the presence of dysmorphic neurons in Type II FCDs can create more pronounced alterations in cortical or subcortical signal, the subtle GM-WM boundary abnormalities are more challenging to detect on MR, particularly in Type I FCDs. We propose that the theoretical basis for 3D-EDGE should lead to increased sensitivity for detection of more subtle changes in T1 relaxation caused by cell disturbances along the normal GM-WM boundary and, therefore, higher FCD detection rate.

2.2. Clinical scans

The study was approved by the Mayo Clinic Institutional Review Board. 3D-EDGE images were obtained as the first inversion image of an MP2RAGE acquisition in a 3 T epilepsy protocol over one year. All scans were reviewed as part of an epilepsy multidisciplinary conference by one of two board-certified neuroradiologists with expertise in epilepsy imaging (E.H.M. and V.G.) and cases with typical imaging findings plus surgical or electrophysiologic evidence of focal epilepsy related to FCD were identified at the time of initial multidisciplinary evaluation. Images were obtained on a 3 T Siemens Skyra or Vida (Siemens Healthineers AG, Erlangen, Germany) using a 32-channel head coil or 64-channel head and neck coil. A Magnetization-Prepared Rapid Gradient-Echo (MP-RAGE) sequence was utilized with two TIs of 700 ms and 2500 ms with a flip angle of 4° and 5° , respectively. Other key parameters are: repetition time (TR) = 5 s, echo time (TE) = 2.98 ms, isotropic resolution of $1 \times 1 \times 1$ mm, receiver bandwidth = 240 Hz/Px, echo spacing = 7.1 ms, turbo factor = 176, and GRAPPA = 3. The total acquisition time was 8:22. The 3D-EDGE image was the first inversion image (TI = 700 ms).

The most representative MR images were selected for purposes of signal and contrast analysis for each case. The mean subcortical signal intensity of the abnormality was calculated and compared to the mean normal WM signal using 3D-EDGE, FLAIR, and MP2RAGE sequences. For two patients with a “transmantle sign,” the mean signal intensity of the linear band extending to the ependymal surface was also compared to mean normal WM for each sequence. One patient also had a double inversion recovery (DIR) sequence for which the mean signal of the transmantle sign and subcortical white matter was also compared to 3D-EDGE and MP2RAGE. Since noise in MP2RAGE is not easily assessed due to the artificial background noise, as well as the fact that the noise in MP2RAGE is an inherent function of the INV1 image itself, we used a modified contrast ratio to assess lesion conspicuity by calculating the absolute value of the percentage signal difference between the lesion and normal white matter. Contrast ratios were compared between the 3D-EDGE, FLAIR, and MP2RAGE using a Mann-Whitney test. After Bonferroni correction, statistical significance was determined at $p < 0.017$.

2.3. 3D-EDGE optimization

For optimizing the 3D-EDGE sequence, MR scans from two normal volunteers were acquired on a 3 T Siemens Vida using a 64-channel phased-array head and neck coil. An MP-RAGE sequence was utilized and a non-selective inversion pulse with inversion times (TI) varying from 500 to 650 ms with a flip angle of 4° and TI of 425–550 ms with a flip angle of 8° . Other key parameters: TR = 2 s, TE = 2.66 ms, isotropic resolution of $1 \times 1 \times 1$ mm, receiver bandwidth = 270 Hz/Px, echo spacing = 6.38 ms, and turbo factor = 154. To test a range of inversion times in feasible imaging time, a high acceleration factor of GRAPPA = 3 and slice partial Fourier = $7/8$ was used for the optimization testing. The resultant acquisition time was 3:22 min.

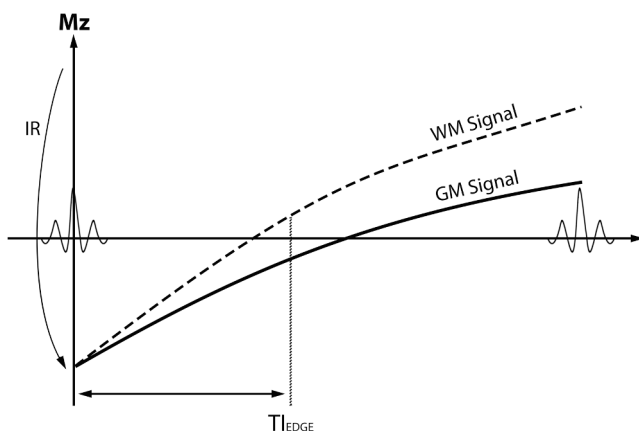


Fig. 1. MRI sequence diagram illustrating the principles underlying the EDGE contrast. After the inversion recovery (IR) pulse is applied, magnetization recovery in the gray matter (GM) and white matter (WM) occurs at different rates. At the EDGE inversion time (TI_{EDGE}), WM and GM have equal signal but at opposite phases (positive versus negative, respectively). As such, voxels with a mixture of GM and WM (e.g., at the GM-WM boundary) will have cancellation of longitudinal magnetization producing an area of signal void.

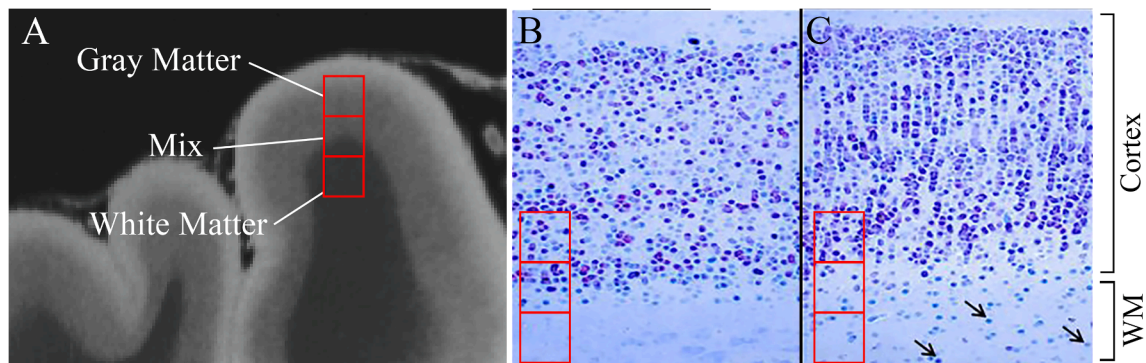


Fig. 2. Theory of focal cortical dysplasia (FCD) detection with 3D-EDGE contrast. (A) Hypothetical MRI voxels (red squares) may contain entirely gray matter, white matter (WM), or a mixture. (B) Comparison to histological illustration of a normal gray matter/white matter boundary again shows sampling of gray matter, white matter, and mixture at the boundary. Given the optimized inversion times for normal gray matter and WM, those voxels with a mixture will show signal cancellation. (C) With an FCD, there is alteration in gray matter cell density along the WM boundary and abnormal ectopic neurons within the subcortical WM (arrows) producing a change in the normal inversion times and creating a “thickening” or distortion of the normal boundary line on 3D-EDGE. (For interpretation of the references to colour in this figure legend, the reader is referred to the web version of this article.)

2.4. Data analysis

All images for each subject were co-registered and masks of GM and WM were generated using the segment function of Statistical Parametric Mapping (SPM) v12 (<https://www.fil.ion.ucl.ac.uk/spm>). The resultant masks were applied to each image to generate a mean signal intensity of both the GM and WM. Signal intensity of GM and WM were plotted versus inversion time (TI) for both FA = 4° and 8°. The “ideal” inversion time should produce similar mean signal intensity in both the GM and WM to optimize visualization of the signal cancellation only at the GM-WM junction.

3. Results

3.1. Clinical scans

Five patients with localized epilepsy and MRI positive findings typical of FCD with electrophysiological correspondence were identified. Four of five cases had previously been interpreted as “normal” prior to acquiring 3D-EDGE on which the abnormalities were first identified upon multidisciplinary review. In all cases, the contrast ratio for the subcortical region and the transmantle sign (present in two cases) was greater on 3D-EDGE images (Fig. 3) compared to MP2RAGE (98% vs 17%; $p = 0.0006$) and FLAIR (98% vs 19%; $p = 0.0006$). There was no significant difference in contrast ratio between the MP2RAGE and FLAIR (17% vs 19%; $p = 0.9$). DIR imaging was also available in one case with a transmantle sign with improved contrast ratio compared to FLAIR (38%

vs 19%), but 3D-EDGE had a greater contrast ratio than DIR (95% vs 38%).

Since the focus of the manuscript is on the technical aspects of the sequence, we include a summary of the identified patients. Patient 1 was a 54-year-old woman with a TSC2 mutation and seizure onset at 20 years of age. Multiple prior outside MRIs were reported as normal. Repeat exam, including DIR and 3D-EDGE, revealed findings consistent with a type IIb left frontal FCD (Fig. 4A & B). Patient 2 was a 29-year-old man with seizure onset at 23 years of age manifested as focal impaired awareness with episodes of focal to bilateral tonic-clonic seizures lateralizing to the right frontal lobe. Initial outside MRI revealed a suspicious lesion in the right posterior frontal lobe with imaging features typical of a type IIb FCD (Fig. 4C-E). Patient 3 was a 17-year-old girl with seizure onset at 15 years of age manifested with gelastic and hypermotor features and no impaired awareness that particularly arose out of sleep. Ictal onset was from the right frontal lobe. At least 4 prior MRIs had been interpreted as normal. 3D-EDGE images revealed a focal thickening of the normal junctional stripe in the right cingulate cortex that was nearly imperceptible on other sequences (Fig. 5). Patient 4 was a 31-year-old with onset of seizures at 2 years of age. The seizures evolved to catamenial focal aware seizures with subjective feeling of “doom” and hypermotor features with rare focal to bilateral convulsive seizures. In epilepsy monitoring, the captured events were noted as nocturnal hypermotor seizures and possible pure ictal aphasia that were reproducible with stimulation of the same onset zone. Imaging revealed a lesion with typical features of FCD in the right frontal pars opercularis (Fig. 6A & B) with subsequent FDG PET-MRI showing a corresponding area of hypometabolism. Patient 5 was 62-year-old woman with well-controlled epilepsy referred for unrelated medical reasons. Per report, she had MRI-negative epilepsy described as hypermotor features without impaired awareness, but further details were not available. A left frontal lesion was subsequently identified (Fig. 6C & D), but her epilepsy continued to be managed in her home city.

3.2. 3D-EDGE optimization

Initial visual inspection by two board-certified neuroradiologists identified TI = 525 at FA = 4° and TI = 425 at FA = 8° as the optimal contrast. The “ideal” contrast was produced by the smallest signal difference between GM and WM, which best highlighted the boundary at the GM/WM junction (Fig. 7A-C). This contrast was also confirmed by quantitative analysis (Fig. 7D & E), which found the same TIs to most closely match GM and WM mean signal intensity. At the lower range of TIs evaluated, WM signal decreased in correlation with decreasing TI, while GM signal increased (anti-correlated) with decreasing TI. GM and

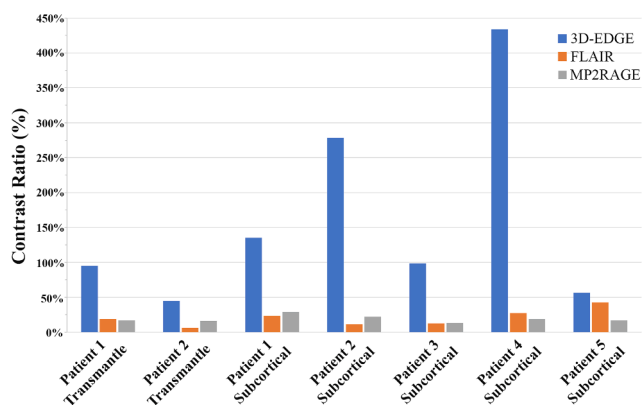


Fig. 3. Difference in contrast ratio of lesions in the 5 patients between 3D-EDGE and typical epilepsy sequences, FLAIR and MP2RAGE.

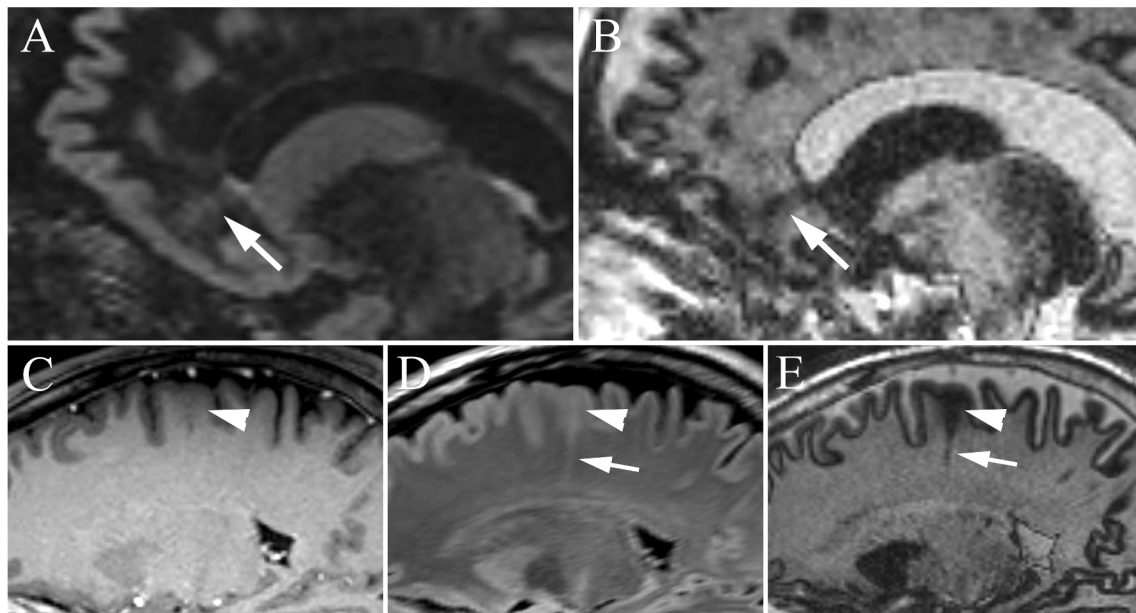


Fig. 4. MRI of focal cortical dysplasia (FCD) in two patients. In Patient 1, sagittal DIR (A) and 3D-EDGE (B) revealed left frontal FCD with transmantle sign (arrow) extending to the ependymal surface of the frontal horn. The disorganization and blurring in the cortex is much better appreciated on the 3D-EDGE image where the boundary line at the gray matter-white matter junction is blurred. In Patient 2, subtle blurring of the gray matter-white matter junction (arrowhead) is present on the MPRAGE image that is more apparent on FLAIR, as well as a “transmantle sign” with a radial band extending to the ependymal surface (arrow). The contrast of both the junctional blurring and subcortical signal change, as well as the transmantle band is greater on the corresponding 3D-EDGE image.

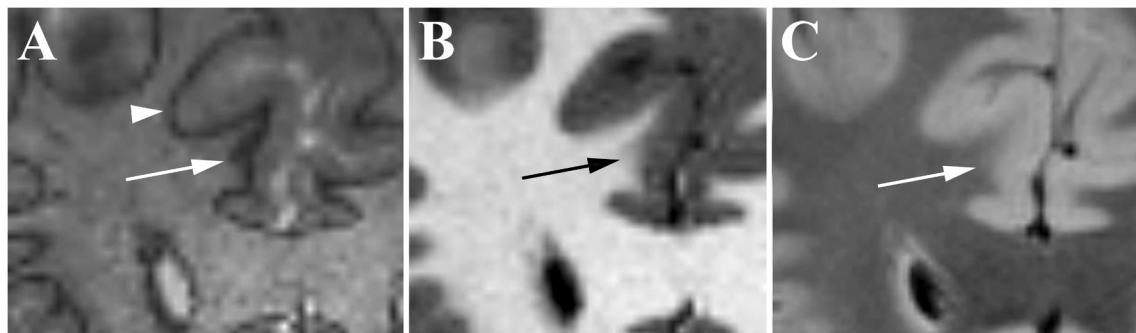


Fig. 5. FCD in patient 3. Four prior MRIs had been interpreted as normal; however, coronal 3D-EDGE (A) image reveals a focal thickening of the junctional band in the right cingulate (arrow), compared to the normal thin junctional band (arrowhead), that is nearly imperceptible on MP2RAGE (B) and FLAIR (C) images.

WM signal intensity curves intersected at $TI = 525$ ms for $FA = 4^\circ$ and intersected at $TI = 425$ for $FA = 8^\circ$.

While integrating 3D-EDGE as the first inversion of an MP2RAGE acquisition may be of practical benefit, the final parameters for a standalone 3D-EDGE sequence at 3 T with a high density phased-array head coil were determined as: a non-selective inversion pulse with $TI = 442$ ms, flip angle of 8° , $TR = 2$ s, $TE = 2.66$ ms, isotropic resolution of $1 \times 1 \times 1$ mm, bandwidth = 270 Hz/Px, echo spacing = 6.4 ms, turbo factor = 154, GRAPPA = 2, and slice partial Fourier = 7/8 with a resultant acquisition time of 4:32. The difference in TI from the test sequence is due to the change of acceleration factor from 3 to 2.

4. Discussion

In this study, we describe 3D-EDGE MRI as a novel application of T1 inversion-recovery for creating high-contrast GM-WM junctional images. Microarchitecture alterations, such as cortical dyslamination in deeper cortical layers, lead to widening or blurring of the GM-WM boundary. Ectopic neurons at the GM-WM boundary and hypomyelination and gliosis in white matter result in averaging of T1 relaxation to an intermediate value between GM and WM in FCD voxels. With an

appropriate TI, this averaging of T1 relaxation leads to nulling of MR signal not only in normal junctional voxels, but also in voxels containing FCD and white matter with increased neuronal density. A similar mechanism leads to signal dropout in transmantle bands of type IIB FCD.

By providing a nearly six-fold increase in contrast ratio at the GM-WM junction in FCD compared to MP2RAGE and FLAIR, 3D-EDGE holds considerable promise in increased detection of FCD. In our series, 3D-EDGE allowed for superior detection and size estimation of FCD with a wide range of appearances compared to FLAIR and DIR. 3D-EDGE produced superior definition of the GM-WM boundary and abnormalities of transition than MP2RAGE. This advantage makes 3D-EDGE particularly valuable in detection of type I FCD. In type II FCD, there is abnormal neuronal and glial proliferation in the cortex (including balloon cells and giant dysmorphic neurons) and radial extensions of abnormal neurons in underlying hypomyelinated white matter (Blumcke et al., 2011). These histologic features facilitate its detection on MRI by causing thickening and T2 prolongation in the cortex and a transmantle sign in the WM. In contrast, type I FCD is characterized by cortical dyslamination without thickening, and presence of ectopic neurons in the underlying WM (Blumcke et al., 2011). These histologic alteration manifest primarily by subtle blurring of the GM-WM junction

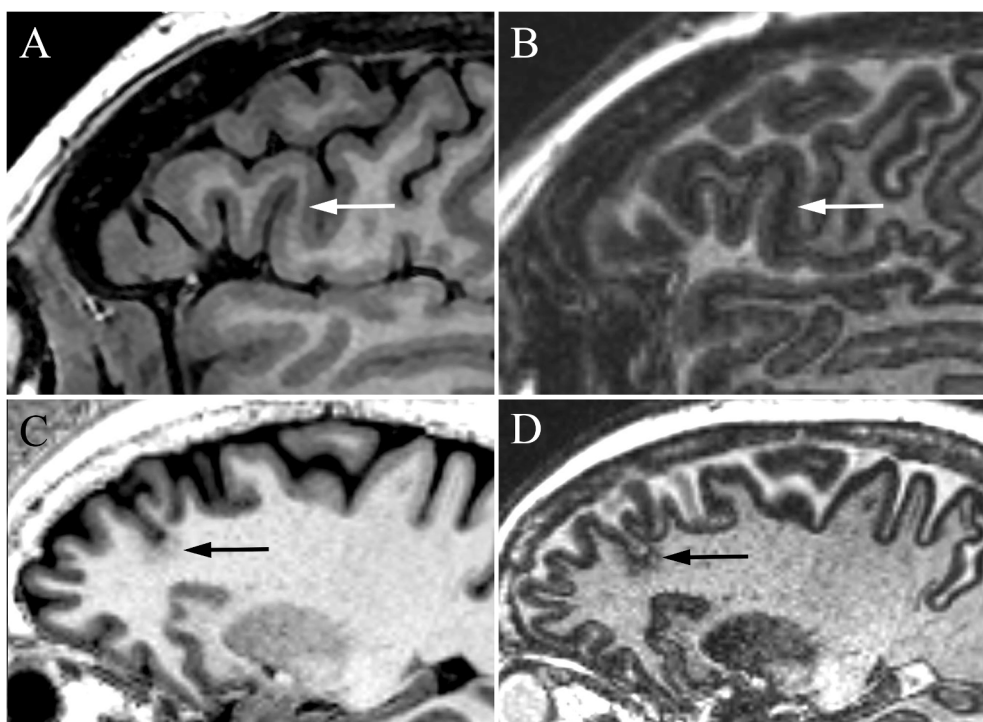


Fig. 6. Example focal cortical dysplasia in two patients. (A) In Patient 4, prior sagittal T1-weighted brain volume imaging (BRAVO) shows very subtle decreased subcortical white matter signal in the right pars opercularis (arrow) that is readily apparent on the subsequent 3D-EDGE (B) image with loss of the normal gray matter-white matter junctional stripe. In Patient 5, sagittal MP2RAGE (C) shows subtle blurring of the gray matter-white matter junction (arrow) that was not visualized on prior MPRAGE (not shown), but shows greater contrast on the sagittal 3D-EDGE (D).

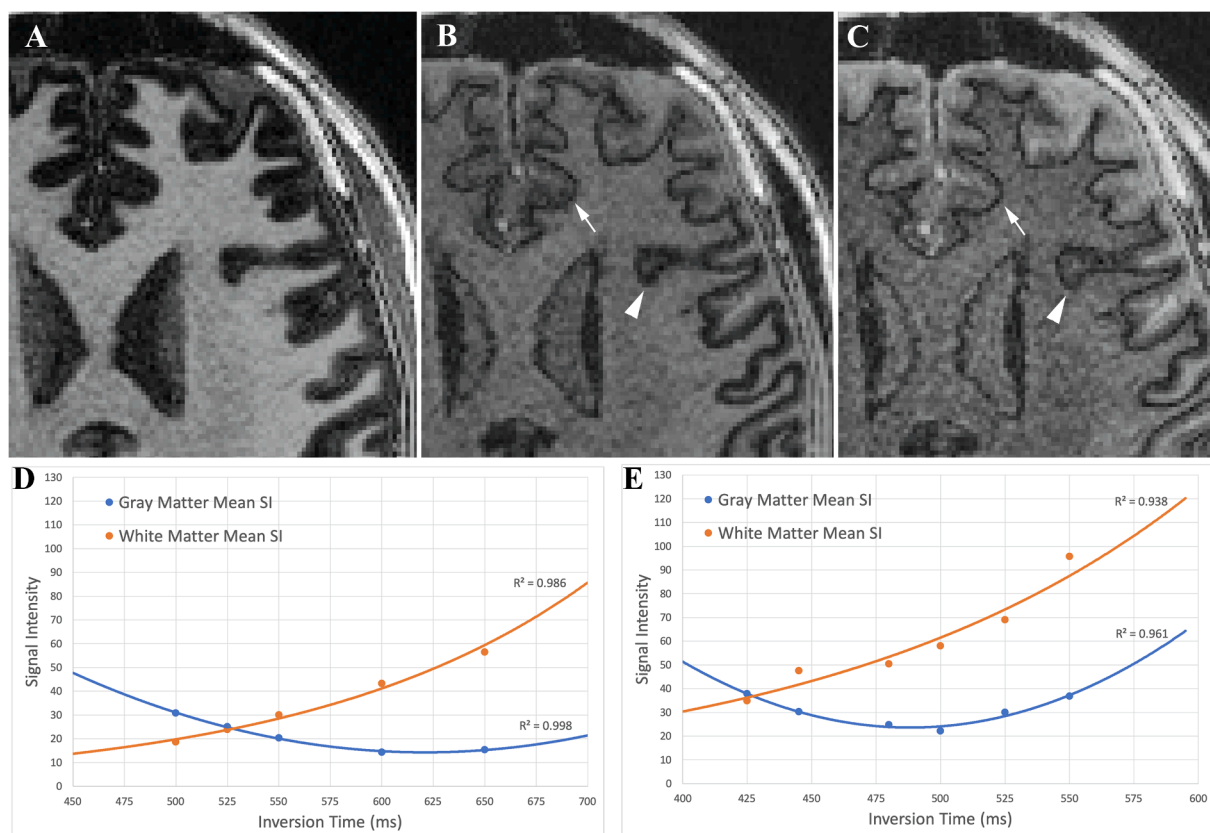


Fig. 7. Effect of changing inversion time (TI) on 3D-EDGE contrast. Example images with flip angle of 8° and varying TI. (A) At a longer TI of 550 ms, gray matter and white matter show dramatic differences in signal intensity. (B) At the shorter TI of 445 ms, cortical signal intensity is brought closer to that of white matter highlighting the boundary line (arrow) in parts of the brain, but with some residual areas of incomplete cortical signal optimization, giving a thickened appearance (arrowhead). (C) Reducing TI to 425 ms creates more uniform cortical signal and 3D-EDGE boundary line (arrowhead) at the cost of slight reduction in SNR. The effect of inversion time on gray matter and white matter signal intensity is shown for (D) flip angle of 4° and (E) flip angle of 8°.

and smearing of the underlying WM on T1-weighted MRI sequences such as MPRAGE or MP2RAGE.

Despite major improvement in SNR and resolution in MRI of epilepsy, detection of type I FCD remains quite challenging, reflected by a preponderance of type II FCDs in surgical series (Bien et al., 2013). The majority of surgically confirmed type I FCD remain undetectable on MRI even upon retrospective review (Wang et al., 2015). The intrinsic limitation of CNR in current MRI sequences, even those with higher GM-WM contrast such as MP2RAGE, lies in the underlying strategy aimed at maximizing the contrast between GM and WM. Due to relatively small differences between T1 and T2 of GM and WM, there is a theoretical limit for the achievable contrast at their boundary. 3D-EDGE is an entirely novel strategy that does not depend on conventional T1 or T2 contrast, but relies on nulling of the signal exclusively in voxels at the GM-WM boundary and voxels of dysplasia containing a mixture of neurons and WM. Such voxels of nulled signal are readily apparent against the intermediate signal of normal GM and WM. Despite reduction in SNR compared to MP2RAGE, the vastly improved lesion contrast in 3D-EDGE holds promise for substantial improvement in detection of type I FCD. In patient 3, focal widening of the dark GM-WM boundary was much more conspicuous than the nearly undetectable blurring of this interface on MP2RAGE and FLAIR. In all patients, 3D-EDGE rendered the FCD much more evident by providing a substantial increase in contrast between normal and abnormal WM compared with MP2RAGE.

Another potential advantage of EDGE lies in defining the full extent of the FCD. Failure to remove or ablate the full extent of dysplasia is associated with poor surgical outcomes. Recognizing the extent of the FCD is also critical in both the planning of intracranial EEG implants, as well as also for accurate intraoperative electrocorticography for safe resection of the FCD when located in or near eloquent regions. This advantage was evident in patient 4, in whom the dysplasia extends more anteriorly and was more extensive on 3D-EDGE than can be appreciated on BRAVO and FLAIR.

In addition to sequence modifications, morphometric analysis programs (MAP) have been utilized to increase the detection rate of FCD over manual evaluation (Wagner et al., 2011). While MAP detection rates for Type IIB are as high as 91%, Type IIA remain elusive with only 65% detection rate (Wagner et al., 2011). Detection rates are even lower for Type I FCDs with nearly half of surgically proven lesions being missed by MAP (Wang et al., 2019), which is likely an underestimate since many Type I FCDs are undetected by MRI resulting in a lower number of patients being offered surgical intervention. Lastly, despite the reported sensitivity of MAP, the rate of false positives is extremely high with one study showing 27% of normal controls having a potential MAP abnormality, which was similar to an epilepsy cohort where 27% of patients had at least one presumed false positive on MAP.16 The accuracy of MAP is thus limited by the CNR of the MR images, as the area under the ROC curve of MAP-based detection is a direct function of the GM-WM contrast. Therefore, 3D-EDGE has the potential to increase the accuracy of MAP in detection of FCD by increasing sensitivity, as well as lowering the false positive rate.

Several limitations of the sequence are noteworthy. First, due to the nature of the tissue signal nulling, the sequence has an inherently low SNR. Despite this, the advantage of substantial increase in contrast ratio seemingly negates this SNR penalty in evaluation for FCD. More aggressive acceleration techniques with high SNR penalty makes further reduction of scan times challenging. Secondly, due to variation in B1 field homogeneity and flip angle evolution, it is challenging to attain optimal GM and WM signal uniformly throughout the brain. As such, we optimized the sequence parameters to maximize this boundary effect within the frontal and temporal lobes given the rate of symptomatic FCD in these locations. Future modifications to the pulse sequence and parallel transmission are needed to generate a more uniform contrast throughout the brain. Lastly, in this technical manuscript, we did not attempt to assess comparative sensitivity and specificity of the 3D-EDGE

sequence, but rather present examples of its superiority in contrast properties in a few cases identified through multidisciplinary review. More data are clearly needed to precisely assess the accuracy and added benefit of the 3D-EDGE sequence in detection of FCD.

5. Conclusions

In summary, we have proposed a novel MRI sequence, 3D-EDGE, that provides improved characterization of the GM-WM boundary through increased sensitivity for changes in normal T1 relaxation using opposed GM-WM phases. In a small cohort of epilepsy patients, the contrast for FCD detection was significantly higher than existing commonly used sequences, including MP2RAGE, FLAIR, and DIR. In particular, we believe this sequence holds promise to increase detection of more elusive Type I and Type IIA FCDs that are notoriously challenging to detect and result in poor epilepsy outcomes.

Funding

This research did not receive any specific grant from funding agencies in the public, commercial, or not-for-profit sectors.

CRedit authorship contribution statement

Erik H. Middlebrooks: Conceptualization, Methodology, Formal analysis, Investigation, Writing - original draft, Writing - review & editing, Visualization. **Chen Lin:** Conceptualization, Methodology, Formal analysis, Investigation, Writing - original draft, Writing - review & editing, Visualization. **Erin Westerhold:** Methodology, Investigation, Writing - review & editing. **Lela Okromelidze:** Formal analysis, Investigation, Writing - review & editing. **Prasanna Vibhute:** Conceptualization, Methodology, Writing - review & editing. **Sanjeet S. Grewal:** Conceptualization, Methodology, Investigation, Writing - review & editing. **Vivek Gupta:** Conceptualization, Methodology, Investigation, Writing - original draft, Writing - review & editing.

Declaration of Competing Interest

The authors declare that they have no known competing financial interests or personal relationships that could have appeared to influence the work reported in this paper.

References

- Bien, C.G., Szinay, M., Wagner, J., Clusmann, H., Becker, A.J., Urbach, H., 2009. Characteristics and surgical outcomes of patients with refractory magnetic resonance imaging-negative epilepsies. *Arch. Neurol.* 66 (12), 1491–1499.
- Bien, C.G., Raabe, A.L., Schramm, J., Becker, A., Urbach, H., Elger, C.E., 2013. Trends in presurgical evaluation and surgical treatment of epilepsy at one centre from 1988–2009. *J. Neurol. Neurosurg. Psychiatry* 84 (1), 54–61.
- Blackmon, K., Kuzniecky, R., Barr, W.B., et al., 2015. Cortical gray-white matter blurring and cognitive morbidity in focal cortical dysplasia. *Cereb. Cortex* 25 (9), 2854–2862.
- Blumcke, I., Thom, M., Aronica, E., et al., 2011. The clinicopathologic spectrum of focal cortical dysplasias: a consensus classification proposed by an ad hoc Task Force of the ILAE Diagnostic Methods Commission. *Epilepsia* 52 (1), 158–174.
- Boulby, P.A., Symms, M.R., Barker, G.J., 2004. Optimized interleaved whole-brain 3D double inversion recovery (DIR) sequence for imaging the neocortex. *Magn. Reson. Med.* 51 (6), 1181–1186.
- Chen, X., Qian, T., Kober, T., et al., 2018. Gray-matter-specific MR imaging improves the detection of epileptogenic zones in focal cortical dysplasia: a new sequence called fluid and white matter suppression (FLAWS). *NeuroImage Clin.* 20, 388–397.
- De Ciantis, A., Barba, C., Tassi, L., et al., 2016. 7T MRI in focal epilepsy with unrevealing conventional field strength imaging. *Epilepsia* 57 (3), 445–454.
- Engel Jr., J., McDermott, M.P., Wiebe, S., et al., 2012. Early surgical therapy for drug-resistant temporal lobe epilepsy: a randomized trial. *JAMA* 307 (9), 922–930.
- Immonen, A., Jutila, L., Muraja-Murro, A., et al., 2010. Long-term epilepsy surgery outcomes in patients with MRI-negative temporal lobe epilepsy. *Epilepsia* 51 (11), 2260–2269.
- Lerner, J.T., Salamon, N., Hauptman, J.S., et al., 2009. Assessment and surgical outcomes for mild type I and severe type II cortical dysplasia: a critical review and the UCLA experience. *Epilepsia* 50 (6), 1310–1335.

- Marques, J.P., Kober, T., Krueger, G., van der Zwaag, W., Van de Moortele, P.F., Gruetter, R., 2010. MP2RAGE, a self bias-field corrected sequence for improved segmentation and T1-mapping at high field. *Neuroimage* 49 (2), 1271–1281.
- Middlebrooks, E.H., Quisling, R.G., King, M.A., et al., 2017. The hippocampus: detailed assessment of normative two-dimensional measurements, signal intensity, and subfield conspicuity on routine 3T T2-weighted sequences. *Surg. Radiol. Anat.* 39 (10), 1149–1159.
- Middlebrooks, E.H., Ver Hoef, L., Szafarski, J.P., 2017. Neuroimaging in epilepsy. *Curr. Neurol. Neurosci. Rep.* 17 (4), 32.
- Phal, P.M., Usmanov, A., Nesbit, G.M., et al., 2008. Qualitative comparison of 3-T and 1.5-T MRI in the evaluation of epilepsy. *AJR Am. J. Roentgenol.* 191 (3), 890–895.
- Shi, J., Lacuey, N., Lhatoo, S., 2017. Surgical outcome of MRI-negative refractory extratemporal lobe epilepsy. *Epilepsy Res.* 133, 103–108.
- Wagner, J., Weber, B., Urbach, H., Elger, C.E., Huppertz, H.J., 2011. Morphometric MRI analysis improves detection of focal cortical dysplasia type II. *Brain* 134 (Pt 10), 2844–2854.
- Wang, Z.I., Jones, S.E., Jaisani, Z., et al., 2015. Voxel-based morphometric magnetic resonance imaging (MRI) postprocessing in MRI-negative epilepsies. *Ann. Neurol.* 77 (6), 1060–1075.
- Wang, W., Lin, Y., Wang, S., et al., 2019. Voxel-based morphometric magnetic resonance imaging postprocessing in non-lesional pediatric epilepsy patients using pediatric normal databases. *Eur. J. Neurol.* 26 (7), 969–e971.